Heliyon 10 (2024) e27380

Contents lists available at ScienceDirect

Heliyon

journal homepage: www.cell.com/heliyon

Research article

# Changes in subclinical cardiac abnormalities 1 Year after recovering from COVID-19 in patients without clinical cardiac findings

Haitao Wang [a,1], Wei Deng [b,1], Yang Zhang [c,1], Jinxiu Yang [b], Zhen Wang [b], Bin Liu [b], Yuchi Han [d], Yongqiang Yu [b,***], Ren Zhao [e,**], Xiaohu Li [b,*]

[a] Department of Radiology, No.2 People's Hospital of Fuyang City, Fuyang, Anhui, China
[b] Department of Radiology, The First Affiliated Hospital of Anhui Medical University, Research Center of Clinical Medical Imaging, Anhui Province Clinical Image Quality Control Center, Hefei, Anhui Province, No. 218 Jixi Road, Hefei, 230022, China
[c] Department of Radiology, Fuyang People's Hospital, Fuyang, 236015, Anhui Province, China
[d] Cardiovascular Division, Wexner Medical Center, College of Medicine, The Ohio State University Medical Center, Columbus, OH, USA
[e] Department of Cardiology The First Affiliated Hospital of Anhui Medical University,Anhui, China

A B S T R A C T

*Aim:* To evaluate the subclinical cardiac involvement in COVID-19 patients without clinical cardiac evidence using cardiac MR imaging.
*Material and methods:* Participants recovered from COVID-19 without cardiac symptoms and no cardiovascular medical history were enrolled in a prospective cohort study. They underwent baseline cardiac MR and follow-up cardiac MR > 300 days after discharge (n = 20). The study also included healthy controls (n = 20). Extracellular volume fraction (ECV), native T1, and 2D strain data were assessed and compared.
*Results:* The ECV values of participants at baseline [30.0% (28.3%–32.5%)] and at follow-up [31.0% (28.0%–32.8%)] were increased compared to the healthy control group [27.0% (25.3%–28.0%)] (both $p < 0.001$). However, the ECV increase from baseline cardiac MR to follow-up cardiac MR was not significant ($p = 0.378$). There was a statistically significant difference in global native T1 between baseline [1140 (1108.3–1192.0) ms] and follow-up [1176.0 (1113.0–1206.3) ms] ($p = 0.016$). However, no native T1 difference was found between the healthy controls [1160.7 (1119.6–1195.4) ms] and the baseline ($p = 0.394$) or follow-up group ($p = 0.168$). The global T2 was 41(40–42) ms at follow-up which was within the normal range. In addition, We found a recovery in 2D GLS among COVID-19 participants between baseline and follow-up [-12.4(-11.7 to −14.3)% vs. −17.2(-16.2 to −18.3)%; $p < 0.001$].
*Conclusion:* Using cardiac MR myocardial tissue and strain imaging parameters, 35% of people without cardiac symptoms or clinical evidence of myocardial injury still had subclinical myocardial tissue characteristic abnormalities at 300 days, but 2D GLS had recovered.

## 1. Introduction

It has been reported that COVID-19 patients developed a series of cardiovascular (CV) abnormalities beyond the acute phase,

* Corresponding authors. Department of Radiology, The First Affiliated Hospital of Anhui Medical University No.218 Jixi Road, Hefei, Anhui. 230022, China.
** Corresponding author. Department of Cardiology, The First Affiliated Hospital of Anhui Medical University, No.218 Jixi Road, Hefei, Anhui, 230022, China.
*** Corresponding author. Department of Radiology, The First Affiliated Hospital of Anhui Medical University, No.218 Jixi Road, Hefei, Anhui, 230022, China.
*E-mail addresses:* ayfyyuyongqiang@126.com (Y. Yu), zhaoren@ahmu.edu.cn (R. Zhao), lixiaohu@ahmu.edu.cn (Xiaohu Li).
[1] Haitao Wang, Wei Deng and Yang Zhang contributed equally to this work.

https://doi.org/10.1016/j.heliyon.2024.e27380
Received 23 August 2023; Received in revised form 26 February 2024; Accepted 28 February 2024
Available online 5 March 2024

including arrhythmia, right ventricular dysfunction, myocardial infarction, and myocarditis [1,2]. The high incidence of acute COVID-19-associated cardiac abnormalities warrants long-term surveillance of myocardial injury in convalescent patients [3–5].

Our previous study reported cardiac MR outcomes in the recovered COVID-19 population approximately 180 days after discharge, including myocardial extracellular volume expansion and decreased myocardial strain. The clinical relevance of the cardiac alterations found in COVID-19-convalescing patients was not evident.

We performed cardiac MR on patients who had been discharged for more than 300 days and were willing to participate in longitudinal follow-up. Our purpose of this study was to investigate the progression of subclinical myocardial findings in patients who recovered from COVID-19.

## 2. Materials and methods

### 2.1. Study population

This observational, prospective study was performed at No.2 People's Hospital of Fuyang City from October 2020 to September 2021, patients recovered from COVID-19 who met the following inclusion criteria were sequentially enrolled (n = 32): (1) Subjects who had confirmed SARS-CoV-2 infection by reverse transcription polymerase chain reaction swab test; (2) No cardiac symptoms at any time, including syncope, palpitations, chest pressure or chest pain, and no shortness of breath after discharge; (3) Normal serum markers including brain natriuretic peptide (BNP), cardiac troponin I (TnI), lactate dehydrogenase (LDH), creatine kinase-MB (CK-MB), and creatine kinase (CK). (4) No abnormalities on ECG. (5) Had baseline cardiac MR within 150 days of discharge. The exclusion criteria are: (1) A history of cardiac disease, such as myocarditis, vascular disease, stroke, diabetes, hypertension, coronary artery disease, or myocardial infarction; (2) A history of aneurysm clips, or shrapnel injury and anaphylactic reactions to cardiac MR contrast agents; (3) Poor quality cardiac MR. (4) Patients who were discharged from the hospital <300 days. (Fig. 1). Healthy controls whose age- and sex-matched those of recovered patients were randomly selected from the database by matching these covariates directly [6]. These healthy controls had no history of cardiovascular disease and were previously enrolled and had cardiac MR examinations at our institution. The study was approved by our local ethics institutional review board (#PJ2020–02–12), and all participants gave written consent.

## 3. Cardiac MR protocol

Cardiac MR was performed using a clinical 3T scanner (Skyra, Siemens Healthcare, Germany). A stack of consecutive parallel short-axis slices covering the entire left ventricle (LV) and right ventricle (RV), and three LV long-axis slices (2,3,4 chamber views) were acquired using balanced steady state-free precession (SSFP). The parameters are as follows: field of view (FOV), 340 × 380 mm; repetition time (TR)/echo time (TE), 3.4/1.4 ms; matrix size: 202 × 182 mm; voxel size 1.6 × 1.6 × 8.0 mm; bandwidth, 962 Hz/Px; flip angle (FA), 47°; slice thickness, 8 mm; slice gap, 2 mm. LGE images were performed approximately 10–15 min after intravenous injection of gadolinium-DTPA at a dose of 0.15 mmol/kg, using the phase-sensitive inversion recovery gradient echo sequence (FOV, 340 × 380 mm; matrix size, 256 × 224 mm; voxel size, 1.3 × 1.3 × 8.0 mm; bandwidth 781Hz/Px; TR, 5.2 ms; TE, 1.24 ms; FA, 55°). Inversion time was individually adjusted to null the myocardium. Native and post-contrast T1 mapping were obtained with typical

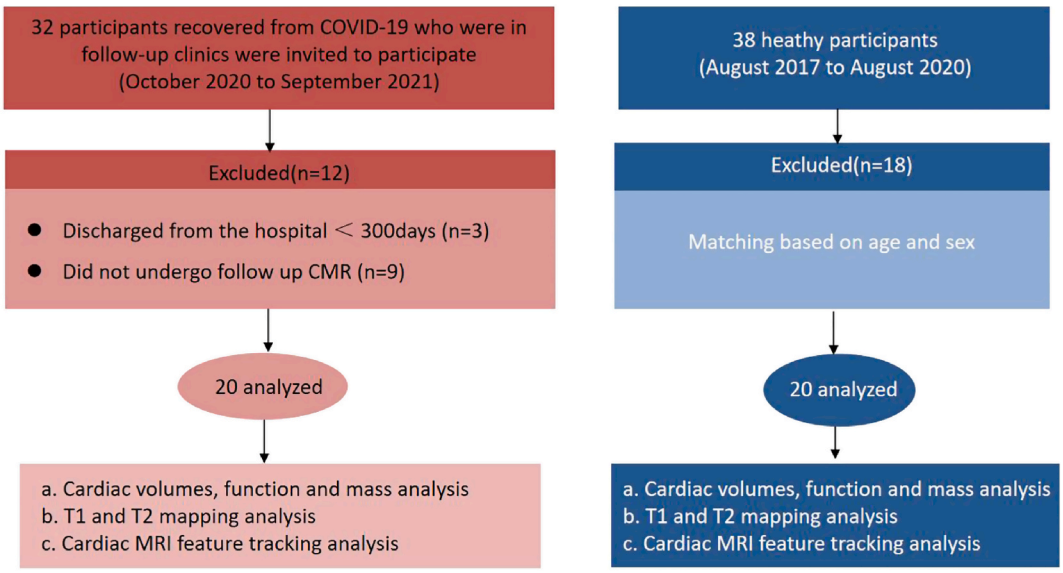


**Fig. 1.** Flowchart of participant enrollment.

parameters at the basal, mid, and apical levels of the LV short axis using the MOLLI sequence (protocols 5(3)3 and 4(1)3(1)2, respectively), before and 15–20 min after venous contrast injection, respectively [7,8]. The scanning parameters are as follows: FOV, 340 × 380 mm; matrix size, 192 × 172 mm; voxel size, 1.3 × 1.3 × 8.0 mm; bandwidth, 1085 Hz/Px; TR/TE, 3.8/1.2 ms; FA, 35°; slice thickness, 8 mm. T2 mapping was performed at the same slice location as T1 mapping using a T2 prepared SSFP sequence (T2 prep duration, 0, 24, 55 ms; FOV, 340 × 380 mm; matrix size, 256 × 224 mm; voxel size, 1.3 × 1.3 × 8.0 mm; bandwidth 781Hz/Px; TR, 208 ms; TE, 1.24 ms; FA, 12°).

### 3.1. Imaging analysis

The cardiac MR data were analyzed using the commercially available post-processing software (CVI42, v.5.1, Circle Cardiovascular Imaging, Calgary, Canada). All cardiac MR data were independently assessed by two radiologists (X.L. with 20 years of cardiac MR experience and H.W. with 15 years of cardiac MR experience) who were blinded to all the identifying information. Functional parameters with CVI42 software were automatically analyzed for LV and RV and manually adjusted, including papillary muscle and trabeculation in the ventricular volume. The LGE images were examined independently by the same two observers. The pattern (epicardial, mid-myocardial, endocardial) and the location of the LGE lesion (16 AHA segment) were assessed manually [9]. Global T1 values were obtained on the T1 map with manual adjustment of contours to exclude intracavitary blood pool and epicardial fat as needed. Global T1 values were the averages of the three short-axis slices. Global ECV was calculated in the native T1 and postcontrast Tl of the myocardium and the blood pool, as previously described [9,10]. Hematocrit was measured from venous blood samples collected from each individual within 24 h before cardiac MR.12 Cardiac MR feature tracking (FT) was performed using CVI42 as previously described [11–13].

### 3.2. Inter-and intra-observer Reproducibility

Using the Bland-Altman method, 10 subjects were randomly selected from 60 subjects to evaluate the reliability of 2D strain and T1 values. The intra-observer reliability was performed by repeating measurements after at least one-month interval and blinded to the initial measurement by a radiologist (X.L.). Another radiologist (H.W.) performed an assessment blinded to the first radiologist measurement for inter-observer reliability.

### 3.3. Statistical analysis

SPSS (version 22.0, IBM statistics, Armonk, NY) was used for statistical analysis. Continuous variables are expressed in median with interquartile range, and categorical variables are expressed in counts (percentages). We used Wilcoxon signed-rank test to evaluate the paired comparison of quantitative variables between two cardiac MRs. Mann-Whitney *U* test was used to evaluate the differences

**Table 1**
Clinical characteristics of the study participants.

| Characteristic | Healthy Controls (n = 20) | All COVID-19 Participants Baseline (n = 20) | All COVID-19 Participants Follow-up (n = 20) | [a] P Value | [b] P value | [c] P value |
|---|---|---|---|---|---|---|
| Median Age (years), | 52(35–61) | 46(41–58) | 47(42–59) | 0.968 | 0.776 | <0.001 |
| Men, No. (%) | 10(50%) | 10(50%) | 10(50%) | >0.99 | >0.99 | >0.99 |
| BMI (kg/m$^2$) | 23.8(22.4–25.1) | 25.0(23.6–25.4) | 25.2(23.5–25.4) | 0.055 | 0.062 | 0.854 |
| Heart rate (bpm) | 70(65–75) | 70(65–76) | 68.0(65.5–75.5) | 0.978 | 0.870 | 0.275 |
| Systolic blood pressure (mmHg) | 126(121–130) | 127(122–133) | 125(121–130) | 0.532 | 0.957 | 0.339 |
| Diastolic blood pressure (mmHg) | 84(81–86) | 79(75–87) | 81(75–88) | 0.125 | 0.266 | 0.350 |
| Confirmed SARS-CoV-2 PCR | 0 | 20(100%) | 20(100%) | NA | | NA |
| Duration between discharge to CMR (days) | 0 | 123(108–142) | 339(327–399) | NA | NA | NA |
| Duration between admission to CMR (days) | 0 | 157(141–169) | 377(355–423) | NA | NA | NA |
| Laboratory results | | | | | | |
| White blood cell count ( × 10$^9$/L) | NA | 5.9(5.4–6.3) | 5.9(5.2–6.5) | NA | NA | 0.736 |
| cTnI, ng/mL | NA | <0.01 | <0.01 | NA | NA | NA |
| BNP, pg/mL | NA | 29.5(23.3–34.0) | 26.5(19.0–31.8) | NA | NA | 0.131 |
| LDH (U/L) | NA | 204.0(168.5–224.5) | 198.0(159.8–221.0) | NA | NA | 0.667 |
| CK-MB (U/L) | NA | 11.5(8.3–14.8) | 12.0(7.3–14.0) | NA | NA | 0.159 |
| CK (U/L) | NA | 80(58.0–137.0) | 79.5(63.5–123.3) | NA | NA | 0.765 |

Data are expressed as median (IQR) for continuous variables, and n (%) for categorical variables. P < 00.05 is considered to indicate statistical significance. BMI = body mass index. HR = heart rate. Bpm = PCR = polymerase chain reaction. LDH = lactate dehydrogenase. cTnI = cardiac troponin I. BNP = brain natriuretic peptide. NA = not apply. CK-MB= Creatine kinase-MB. CK= Creatine kinase IQR = interquartile range.

[a] P value statistical difference between Healthy Controls and COVID-19 participants at baseline.

[b] P value statistical difference between Healthy Controls and COVID-19 participants at follow-up.

[c] P value statistical difference between COVID-19 participants at baseline and follow-up.

between two independent samples. Chi-square tests were used to evaluate the differences between categorical variables. $P < 0.05$ was considered statistically significant.

## 4. Results

### 4.1. Participant characteristics

20 participants and 20 healthy controls matched for age [47(42–59) vs. 52(35–61) years, p = 0.776] and sex were included in the study (Fig. 1). Table 1 reports the clinical characteristics and laboratory test results. The time interval between admission or discharge and baseline cardiac MR examination was 157(141–169) and 123(108–142) days. The time interval between admission or discharge and follow-up cardiac MR examination was 377(355–423) and 339(327–399) days (Table 1).

### 4.2. Cardiac MR results

The cardiac morphological and functional parameters are shown in Table 2. The left ventricular end-diastolic volume index at follow-up [61.9(57.0–74.6) mL/m2] was significantly higher than that at the baseline [59.9(55.1–79.2) mL/m2] (p = 0.03). All baseline and follow-up participants with COVID-19 had negative LGE. The ECV values of COVID-19 recovery participants at baseline [30.0% (28.3%–32.5%)] and at follow-up [31.0% (28.0%–32.8%)] were increased compared to the healthy control group [27.0% (25.3%–28.0%)] (both p < 0. 001). However, the ECV increase from baseline cardiac MR to the follow-up examination was not significant (p = 0.378). 55% (11/20) of the baseline participants and 35% (7/20) of the follow-up participants' ECV values were above the upper limit of normal (29%) (Fig. 2).

There was a statistically significant difference in global native T1 between baseline [1140 (1108.3–1192.0) ms] and follow-up [1176.0 (1113.0–1206.3) ms] (p = 0.016). However, no difference in native T1 was found between the healthy controls [1160.7 (1119.6–1195.4) ms] and the baseline (p = 0.394) or follow-up group (p = 0.168). The global T2 was 41(40–42) ms at follow-up which was within the normal range. The representative native T1 mapping images of the patients are shown in Fig. 3.

We found a recovery in 2D GLS among COVID-19 participants between baseline and follow-up [−12.4(−11.7 to −14.3)% vs. −17.2 (−16.2 to −18.3)%; p < 0.001]. There was a significant difference compared to healthy controls at baseline [−15.4(−14.3 to −17.8)% vs. −12.4(−11.7 to −14.3)%; p = 0.001]. There were no significant differences between follow-up participants and healthy controls [−17.2(−16.2 to −18.3) vs. −15.4(−14.3 to −17.8); p = 0.066].

The clinical characteristics and cardiac MR results of the group with increased ECV versus decreased ECV compared to baseline are shown in Table 3. Two patients had no change in ECV compared to baseline data. The median age in ECV-increased group was older than the ECV-decreased group (57(56–61) vs. 44(34–49) years) (p = 0.021). The median length of first-time Covid-19 hospitalizations stay was longer (30(29–40) vs. 27(25–28) days, p = 0.003) days in the ECV-increased group as compared to the ECV-decreased group. Global native T1 (1270.0(1255.0–1292.0) ms) in ECV-increased group was higher compared with the ECV-decreased group (1146.0 (1098.0–1222.0) ms) (p = 0.006).

**Table 2**
Cardiac CMR results at baseline and follow-up examinations.

| Variable | Healthy Controls (n = 20) | Baseline (n = 20) | Follow-up (n = 20) | [a]P Value | [b]P value | [c] P value |
|---|---|---|---|---|---|---|
| LVEF (%) | 63.5(61.6–66.4) | 63.7(59.8–67.1) | 64.5(60.7–66.1) | 0.705 | 0.725 | 0.601 |
| LVEDVi(mL/m2) | 60.9(53.2–66.9) | 59.9(55.1–79.2) | 61.9(57.0–74.6) | 0.607 | 0.176 | 0.030 |
| LV mass index (g/m2) | 55.7(47.4–66.6) | 51.3(44.9–60.5) | 51.9(48.6–58.6) | 0.267 | 0.417 | 0.709 |
| RVEF (%) | 56.1(53.2–58.5) | 53.9(51.2–55.9) | 55.1(50.8–57.9) | 0.152 | 0.317 | 0.247 |
| RVEDVi (mL/m2) | 78.9(67.4–83.5) | 68.2(59.3–86.1) | 68.7(63.5–83.8) | 0.159 | 0.234 | 0.156 |
| Visible myocardial LGE | NA | 0(0) | 0(0) | NA | NA | NA |
| Visible pericardial LGE | NA | 0(0) | 0(0) | NA | NA | NA |
| Pericardial effusion | 0(0) | 0(0) | 0(0) | NA | NA | NA |
| Pleural effusion | 0(0) | 0(0) | 0(0) | NA | NA | NA |
| Global native T1 (ms) | 1160.7(1119.6–1195.4) | 1140(1108.3–1192.0) | 1176.0(1113.0–1206.3) | 0.394 | 0.168 | 0.016 |
| Global ECV (%) | 27.0(25.3–28.0) | 30.0(28.3–32.5) | 31(28.0–32.8) | <0.001 | <0.001 | 0.378 |
| Global T2 (ms) | 41(40–42) | NA | 41(40–42) | NA | NA | NA |
| 2D Strain | | | | | | |
| 2D GLS (%) | −15.4(-14.3−−17.8) | −12.4(-11.7−−14.3) | −17.2(-16.2−−18.3) | 0.001 | 0.066 | <0.001 |
| 2D GCS (%) | −21.9(-20.4−−22.7) | −21.0(-14.3−−23.7) | −21.0(-16.6−−23.3) | 0.291 | 0.262 | 0.433 |
| 2D GRS (%) | 33.7(24.9–39.5) | 20.8(9.7–41.3) | 21.6(14.8–39.1) | 0.130 | 0.068 | 0.279 |

Data are expressed as median (IQR) for continuous variables. P < 00.05 is considered to indicate statistical significance. Baseline: First Cardiac CMR; Follow-up: Second Cardiac CMR. LV: Left ventricular; EF: ejection fraction; EDVi:Left ventricular end-diastolic volume index; RV: right ventricular; GLS: global longitudinal strain; GCS: global circumferential strain; GRS: global radial strain; LGE: late gadolinium enhancement; ECV: extracellular volume fraction; 2D = 2 dimensional.

[a] P value statistical difference between Healthy Controls and COVID-19 participants at baseline.

[b] P value statistical difference between Healthy Controls and COVID-19 participants at follow-up.

[c] P value statistical difference between COVID-19 participants at baseline and follow-up.

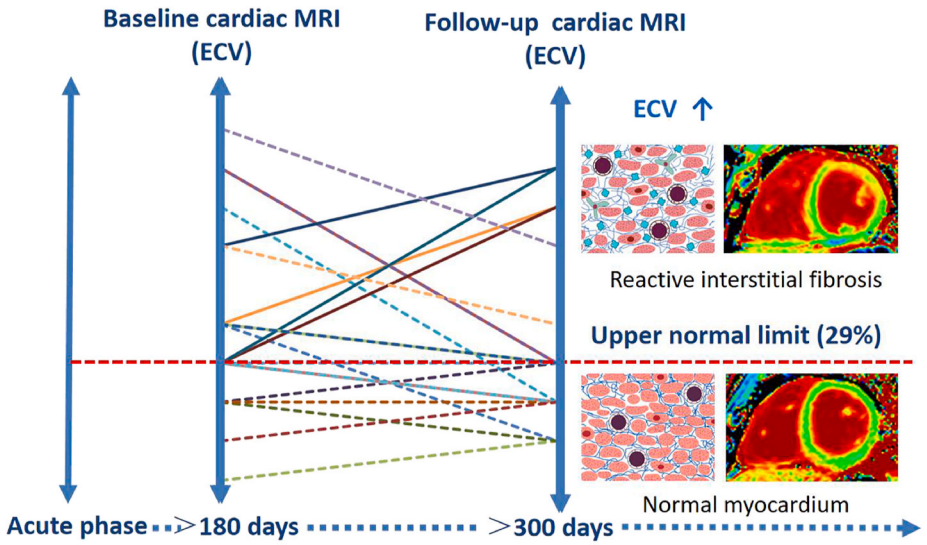


**Fig. 2.** The schematic diagram of myocardial ECV change in the first year after SARS CoV-2 infection. ECV elevation represents reactive interstitial fibrosis and/or edema. ECV reduction may reflect the regression of reactive interstitial fibrosis and/or extracellular interstitial edema.

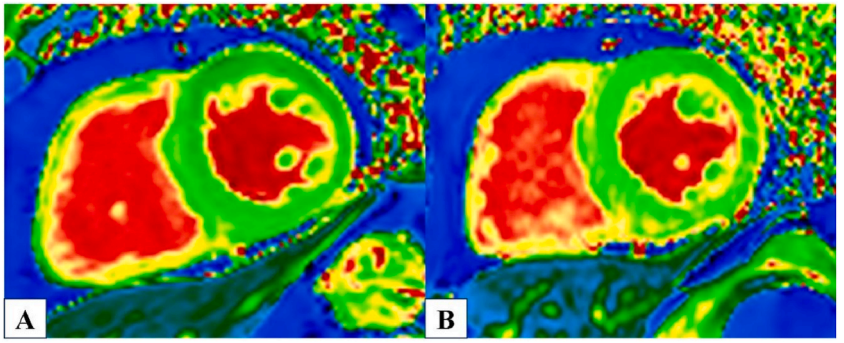


**Fig. 3.** CMR native T1 maps in a 66-year-old with COVID-19 at baseline and a 1-year follow-up. A. Baseline short-axis T1 map image shows normal global native T1 of 1106 ms. B. Follow-up T1 map shows an elevated global native T1 of 1292 ms.

### *4.3. Intra-and inter-observer reliability*

BA plot for intra-observer reliability of the global native T1 was 0.40 ± 0.84 ms, and inter-observer reliability was −0.26 ± 1.42 ms. The intra-observer reliability of the global ECV was −0.17% ± 0.44% and the inter-observer reliability was −0.81% ± 0.65%. BA plot for intra-observer reliability of 2D GLS was 0.02% ± 0.79% and inter-observer reliability of 2D GLS was 0.14% ± 1.03%.

## 5. Discussion

COVID-19's long-term impact on cardiovascular health and mortality has become a global concern [3,14,15]. Davis et al. [16] studied 3762 patients and found that cardiac symptoms including fainting (13%), palpitations (68%), and chest pain (53%) were observed in up to 86% of patients by 7 months from infection.

Cardiac MR is a non-invasive reference standard for cardiac function, structure, and tissue composition which is a potentially valuable diagnostic tool for COVID-19 patients with myocardial injury and cardiac dysfunction [2,9,17–20].

Although COVID-19-related myocarditis is not common, up to 28.8% of patients have reported COVID-19-related cardiovascular abnormalities, which increases concerns about long-term myocardial injury [18,21–25]. So far, studies have reported that 26%–60% of hospitalized patients within 1–5 months after discharge had abnormal cardiac MR findings, including myocardial tissue abnormalities, pericardial abnormalities, functional impairment, or late gadolinium enhancement [3,18]. Recent cardiac MR investigations showed that patients with COVID-19 who are outpatients, including elite athletes, as well as hospitalized patients, may also have cardiac consequences. At present, it is not completely clear how these myocardial changes evolve in convalescent COVID-19 patients without any cardiac abnormalities.

The precision and repeatability, as well as its ability in myocardial tissue characterization are the advantages of using cardiac MR in

**Table 3**
Clinical characteristics and cardiac CMR Results of ECV increase versus decrease groups.

| Characteristic | ECV-increased groups (n = 7) | ECV-decreased groups (n = 11) | P value |
|---|---|---|---|
| Median Age (years) | 57(56–61) | 44(34–49) | 0.021 |
| Men, No.(%) | 4(57%) | 5(45%) | 0.320 |
| BMI (kg/m$^2$) | 25.4(23.6–25.6) | 24.9(23.4–25.3) | 0.363 |
| Heart rate (bpm) | 68(65–76) | 68(67–78) | 0.819 |
| Systolic blood pressure (mmHg) | 125(125–130) | 125(120–130) | 0.482 |
| Diastolic blood pressure (mmHg) | 86(70–88) | 80(75–85) | 0.438 |
| Duration between discharge to cardiac CMR (days) | 338(336–357) | 359(329–418) | 0.497 |
| Duration between admission to cardiac CMR (days) | 380(364–387) | 384(357–445) | 0.751 |
| Average length of Covid-19 hospitalizations stay(days) | 30(29–40) | 27(25–28) | 0.003 |
| Laboratory results | | | |
| White blood cell count ( $\times 10^9$/L) | 5.9(5.0–7.0) | 5.8(5.2–6.5) | 0.554 |
| cTnI, ng/mL | <0.01 | <0.01 | NA |
| BNP, pg/mL | 30.0(19.0–32.0) | 26.0(19.0–30.0) | 0.525 |
| LDH (U/L) | 198.0(165.0–218.0) | 185.0(146.0–236.0) | 0.525 |
| CK-MB(U/L) | 11.0(6.0–14.0) | 12.0(8.0–14.0) | 0.750 |
| CK(U/L) | 107(65.0–142.0) | 78.0(62.0–124.0) | 0.033 |
| Cardiac MRI findings | | | |
| Left ventricular ejection fraction (%) | 60.5(56.4–62.4) | 64.5(61.5–66.3) | 0.069 |
| Left ventricular end-diastolic volume index (mL/m$^2$) | 64.5(60.5–74.6) | 57.9(56.3–74.6) | 0.341 |
| Left ventricular mass index (g/m$^2$) | 52.3(50.3–58.6) | 51.6(45.6–61.5) | 0.856 |
| Right ventricular ejection fraction (%) | 52.6(48.9–55.6) | 57.8(51.6–58.9) | 0.057 |
| Right ventricular end-diastolic volume index (mL/m$^2$) | 74.5(63.8–79.6) | 65.5(61.5–84.6) | 0.525 |
| Global native T1 (ms) | 1270.0(1255.0–1292.0) | 1146.0(1098.0–1222.0) | 0.006 |
| Global ECV (%) | 33.0(28.0–34.0) | 29.0(28.0–29.0) | 0.117 |
| 2D GLS (%) | −17.6(-16.2–−17.9) | −16.9(-16.2–−18.5) | 0.892 |
| 2D GRS (%) | 20.6(19.8–35.6) | 28.6(13.5–40.5) | 0.821 |
| 2D GCS (%) | −18.5(-16.5–−18.5) | −21.5(-15.7–−23.6) | 0.556 |

Data are expressed as median (IQR) for continuous variables. $P < 0.05$ is considered to indicate statistical significance. GLS: global longitudinal strain; GCS: global circumferential strain; GRS: global radial strain; LGE: late gadolinium enhancement; ECV: extracellular volume fraction; 2D: 2 dimensional; CMR: magnetic resonance imaging; BMI: body mass index; HR: heart rate; PCR = polymerase chain reaction; LDH: lactate dehydrogenase; cTnI: cardiac troponin I; BNP: brain natriuretic peptide; NA: not apply; CK-MB: Creatine kinase-MB; CK: Creatine kinase; IQR = interquartile range.

the context of COVID-19 [9,18,19]. We found that 55% (11/20) of the participants had an increase in ECV about 123 days after discharge and 35% (7/20) of the participants had an elevated ECV (>29%) about 339 days after discharge (Fig. 3). These participants had no clinical signs of myocardial damage or cardiac symptoms, and there is no functional or anatomical cardiac impairment (LVEF 64.5(60.7–66.1) % at follow-up vs. 63.7(59.8–67.1) % at baseline) (Fig. 4).

Diffuse interstitial and localized replacement fibrosis are two manifestations of SARS-CoV-2-induced myocarditis [2]. Myocardial scarring with localized replacement fibrosis may be uncommon among individuals with moderate or severe acute COVID-19 infection but no cardiac symptoms or clinical signs, according to our prior study.6 Diffuse myocardial fibrosis, which is defined by the expansion of extracellular space and an excessive buildup of collagen in the extracellular matrix, is typically a reaction to recurrent or unresolved injury and stress [26]. Inflammation leading to repeated injury causes tissue damage and repair under both chronic ischemic and non-ischemic settings, activating innate immune responses with the resultant widespread interstitial fibrosis [26,27]. cardiac MR has been considered the non-invasive method of choice for detecting diffuse myocardial fibrosis by calculating ECV from T1 mapping and hematocrit [9,26]. The pathological remodeling of the myocardium is caused by the inflammatory process of interstitial fibrosis, which is often linked to apoptosis. Apoptosis promotes the accumulation of collagen, resulting in an increase in extracellular volume. Viral infections, which may be latent but can potentially induce or accelerate fibrosis and structural remodeling, often trigger innate immune responses [26]. Chronic infections associated with myocardial fibrosis and cardiac hypertrophy can be evaluated using ECV [3,15,18,26,27].

Since ECV evaluates the overall interstitial space, an elevation in ECV can be a result of fibrous tissue, infiltration, edema, and/or inflammation [26,27]. We observed a decrease in extracellular volume fraction at 1 year in most of the participants who presented with an abnormal ECV at baseline. None of the patients had T2 elevation at 1-year follow-up. One possible explanation for this change is that ECV reflects the regression of extracellular interstitial edema, which was a common finding in COVID-19's autopsy reports [3,18].

Our research has several limitations. Firstly, the sample size of this study is relatively small, and further studies with more patients are needed to confirm the conclusion. Secondly, the relationship between cardiac MR parameters and histology could not be verified due to the lack of myocardial biopsy. Thirdly, there is no follow up of the healthy cohort.

In conclusion, subclinical abnormalities in myocardial tissue are still present in some COVID-19 survivors without cardiac symptoms or overt myocardial injury at one year after recovery. Although all patients had improved subclinical function as shown by myocardial strain, myocardial interstitial alterations remained in some patients. To ascertain the diagnostic significance of these findings and their connection to incident health outcomes, longer-term (>1 year) investigations are needed.

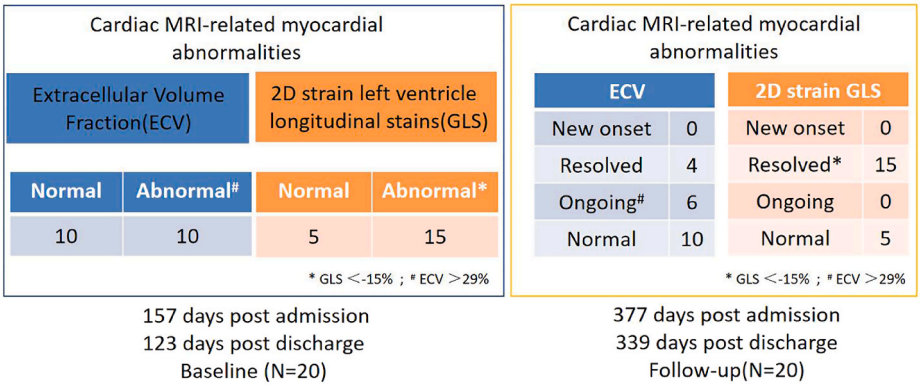


**Fig. 4.** Cardiac MRI-related myocardial abnormalities.

## Funding

This work was supported by the National Natural Science Foundation of China (82371949, 82371959, 82071897, 81970446) and National Science Foundation for Distinguished Young Scholars of the Higher Education Institutions of Anhui Province, China (2022AH020071). Anhui Provincial Natural Science Foundation (2308085Y48, 202304295107020027, 202304295107020028, 202304295107020029) and the Science Foundation of Anhui Provincial Health Commission ( AHWJ2022c007 ) and Natural Science Foundation of Fuyang City (FYZDYF2023LCYX043).

## Data availability statement

The authors declare that the data supporting the findings of this study are available within the paper, a request for more detailed data should be sent to the corresponding authors with the permission of all authors.

## CRediT authorship contribution statement

**Haitao Wang:** Writing – original draft, Resources, Methodology, Investigation, Funding acquisition, Data curation. **Wei Deng:** Writing – original draft, Visualization, Validation, Methodology, Investigation. **Yang Zhang:** Writing – original draft, Methodology, Investigation. **Jinxiu Yang:** Validation, Project administration, Data curation. **Zhen Wang:** Investigation. **Bin Liu:** Project administration, Conceptualization. **Yuchi Han:** Writing – review & editing, Methodology, Formal analysis, Conceptualization. **Yongqiang Yu:** Writing – review & editing, Supervision, Software, Resources, Project administration, Funding acquisition. **Ren Zhao:** Writing – review & editing, Supervision, Resources, Project administration, Methodology. **Xiaohu Li:** Writing – review & editing, Supervision, Software, Resources, Project administration, Methodology, Formal analysis, Data curation, Conceptualization.

## Declaration of competing interest

The authors declare that they have no known competing financial interests or personal relationships that could have appeared to influence the work reported in this paper.

## References

[1] L.H. Ketai, Deciphering the risk of thromboembolism in COVID-19, Radiology 301 (2021) E436–E437, https://doi.org/10.1148/radiol.2021211563.
[2] D. Kravchenko, A. Isaak, S. Zimmer, N. Mesropyan, M. Reinert, A. Faron, C.C. Pieper, A. Heine, M. Velten, J. Nattermann, D. Kuetting, G.D. Duerr, U. I. Attenberger, J.A. Luetkens, Cardiac MRI in patients with prolonged cardiorespiratory symptoms after mild to moderate COVID-19, Radiology 301 (2021) E419, https://doi.org/10.1148/radiol.2021211162. –E425.
[3] B. Raman, D.A. Bluemke, T.F. Lüscher, S. Neubauer, Long COVID: post-acute sequelae of COVID-19 with a cardiovascular focus, Eur. Heart J. 43 (2022) 1157–1172, https://doi.org/10.1093/eurheartj/ehac031.
[4] A.N. Leung, COVID-19 pandemic: the road to recovery, Radiology 304 (2022) 471–472, https://doi.org/10.1148/radiol.220488.
[5] A.K. Luger, T. Sonnweber, L. Gruber, C. Schwabl, K. Cima, P. Tymoszuk, A.K. Gerstner, A. Pizzini, S. Sahanic, A. Boehm, M. Coen, C.J. Strolz, E. Wöll, G. Weiss, R. Kirchmair, G.M. Feuchtner, H. Prosch, I. Tancevski, J. Löffler-Ragg, G. Widmann, Chest CT of lung injury 1 Year after COVID-19 pneumonia: the CovILD study, Radiology 304 (2022) 462–470, https://doi.org/10.1148/radiol.211670.
[6] N. Greifer, E.A. Stuart, Matching methods for confounder adjustment: an addition to the epidemiologist's toolbox, Epidemiol. Rev. 43 (2022) 118–129, https://doi.org/10.1093/epirev/mxab003.
[7] W. Deng, J. Zhang, R. Zhao, Y. Qian, Y. Han, Y. Yu, X. Li, T1 mapping values may Be associated with early myocardial involvement in Young patients with wilson disease, Radiol Cardiothorac Imaging 4 (2022) e220145, https://doi.org/10.1148/ryct.220145.
[8] W. Deng, Y. Xue, Y. Li, S. An, J. Zheng, Y. Qian, X. Yue, Z. Wu, Y. Yu, R. Zhao, X. Li, Normal values of magnetic resonance T1ρ relaxation times in the adult heart at 1.5 T MRI, J. Magn. Reson. Imag. 58 (2023) 477–485, https://doi.org/10.1002/jmri.28506.
[9] E.B. Schelbert, D.R. Messroghli, State of the art: clinical applications of cardiac T1 mapping, Radiology 278 (2016) 658–676, https://doi.org/10.1148/radiol.2016141802.

[10] K. Hanneman, E.T. Nguyen, P. Thavendiranathan, R. Ward, A. Greiser, M.-P. Jolly, J. Butany, I.Y. Yang, M.S. Sussman, B.J. Wintersperger, Quantification of myocardial extracellular volume fraction with cardiac MR imaging in thalassemia major, Radiology 279 (2016) 720–730, https://doi.org/10.1148/radiol.2015150341.
[11] K. Wan, J. Sun, D. Yang, H. Liu, J. Wang, W. Cheng, Q. Zhang, Z. Zeng, T. Zhang, A. Greiser, M.-P. Jolly, Y. Han, Y. Chen, Left ventricular myocardial deformation on cine MR images: relationship to severity of disease and prognosis in light-chain amyloidosis, Radiology 288 (2018) 73–80, https://doi.org/10.1148/radiol.2018172435.
[12] A.A. Kammerlander, C. Donà, C. Nitsche, M. Koschutnik, R. Schönbauer, F. Duca, C. Zotter-Tufaro, C. Binder, S. Aschauer, D. Beitzke, C. Loewe, C. Hengstenberg, D. Bonderman, J. Mascherbauer, Feature tracking of global longitudinal strain by using cardiovascular MRI improves risk stratification in heart failure with preserved ejection fraction, Radiology 296 (2020) 290–298, https://doi.org/10.1148/radiol.2020200195.
[13] J. He, W. Yang, W. Wu, S. Li, G. Yin, B. Zhuang, J. Xu, X. Sun, D. Zhou, B. Wei, A. Sirajuddin, Z. Teng, S. Zhao, F. Kureshi, M. Lu, Early diastolic longitudinal strain rate at MRI and outcomes in heart failure with preserved ejection fraction, Radiology 301 (2021) 582–592, https://doi.org/10.1148/radiol.2021210188.
[14] M. Augustin, P. Schommers, M. Stecher, F. Dewald, L. Gieselmann, H. Gruell, C. Horn, K. Vanshylla, V.D. Cristanziano, L. Osebold, M. Roventa, T. Riaz, N. Tschernoster, J. Altmueller, L. Rose, S. Salomon, V. Priesner, J.C. Luers, C. Albus, S. Rosenkranz, B. Gathof, G. Fätkenheuer, M. Hallek, F. Klein, I. Suárez, C. Lehmann, Post-COVID syndrome in non-hospitalised patients with COVID-19: a longitudinal prospective cohort study, Lancet Reg Health Eur 6 (2021) 100122, https://doi.org/10.1016/j.lanepe.2021.100122.
[15] J.A.C. Lima, D.A. Bluemke, Myocardial scar in COVID-19: innocent marker versus harbinger of clinical disease, Radiology 301 (2021) E434–E435, https://doi.org/10.1148/radiol.2021211710.
[16] H.E. Davis, G.S. Assaf, L. McCorkell, H. Wei, R.J. Low, Y. Re'em, S. Redfield, J.P. Austin, A. Akrami, Characterizing long COVID in an international cohort: 7 months of symptoms and their impact, EClinicalMedicine 38 (2021) 101019, https://doi.org/10.1016/j.eclinm.2021.101019.
[17] M. Gottbrecht, C.M. Kramer, M. Salerno, Native T1 and extracellular volume measurements by cardiac mri in healthy adults: a meta-analysis, Radiology 290 (2019) 317–326, https://doi.org/10.1148/radiol.2018180226.
[18] S.E. Petersen, M.G. Friedrich, T. Leiner, M.D. Elias, V.M. Ferreira, M. Fenski, S.D. Flamm, M. Fogel, R. Garg, M.K. Halushka, A.G. Hays, N. Kawel-Boehm, C. M. Kramer, E. Nagel, N.A.B. Ntusi, E. Ostenfeld, D.J. Pennell, Z. Raisi-Estabragh, S.B. Reeder, C.E. Rochitte, J. Starekova, D. Suchá, Q. Tao, J. Schulz-Menger, D. A. Bluemke, Cardiovascular magnetic resonance for patients with COVID-19, JACC Cardiovasc Imaging 15 (2022) 685–699, https://doi.org/10.1016/j.jcmg.2021.08.021.
[19] P. Pattanayak, D.A. Bluemke, Cardiac MR imaging to probe tissue composition of the heart by using T1 mapping, Radiology 271 (2014) 320–322, https://doi.org/10.1148/radiol.14140287.
[20] C.A. Hanson, A. Kamath, M. Gottbrecht, S. Ibrahim, M. Salerno, T2 relaxation times at cardiac mri in healthy adults: a systematic review and meta-analysis, Radiology 297 (2020) 344–351, https://doi.org/10.1148/radiol.2020200989.
[21] J.A. Luetkens, A. Isaak, C. Öztürk, N. Mesropyan, M. Monin, S. Schlabe, M. Reinert, A. Faron, A. Heine, M. Velten, D. Dabir, C. Boesecke, C.P. Strassburg, U. Attenberger, S. Zimmer, G.D. Duerr, J. Nattermann, Cardiac MRI in suspected acute COVID-19 myocarditis, Radiol Cardiothorac Imaging 3 (2021) e200628, https://doi.org/10.1148/ryct.2021200628.
[22] J. Starekova, D.A. Bluemke, W.S. Bradham, T.M. Grist, M.L. Schiebler, S.B. Reeder, Myocarditis associated with mRNA COVID-19 vaccination, Radiology 301 (2021) E409, https://doi.org/10.1148/radiol.2021211430. –E411.
[23] B. Raman, S. Neubauer, Postvaccine Myocarditis, A risk worth the reward? Radiology 304 (2022) 563–565, https://doi.org/10.1148/radiol.220252.
[24] M. Fronza, P. Thavendiranathan, V. Chan, G.R. Karur, J.A. Udell, R.M. Wald, R. Hong, K. Hanneman, Myocardial injury pattern at MRI in COVID-19 vaccine-associated myocarditis, Radiology 304 (2022) 553–562, https://doi.org/10.1148/radiol.212559.
[25] M.K. Vidula, J. Rajewska-Tabor, J.J. Cao, Y. Kang, J. Craft, W. Mei, P.S. Chandrasekaran, D.E. Clark, A.-M. Poenar, M. Gorecka, M. Malahfji, E. Cowan, J. M. Kwan, S.W. Reinhardt, S. Al-Tabatabaee, P. Doeblin, A.D.M. Villa, I. Karagodin, N. Alvi, P. Christia, N. Spetko, M.P. Cassar, C. Park, L. Nambiar, A. Turgut, M. R. Azad, M. Lambers, T.C. Wong, M. Salerno, J. Kim, M. Elliott, B. Raman, S. Neubauer, C.W. Tsao, G. LaRocca, A.R. Patel, A. Chiribiri, S. Kelle, L.A. Baldassarre, D.J. Shah, S.G. Hughes, M.S. Tong, M. Pyda, O.P. Simonetti, S. Plein, Y. Han, Myocardial injury on CMR in patients with COVID-19 and suspected cardiac involvement, JACC Cardiovasc Imaging 16 (2023) 609–624, https://doi.org/10.1016/j.jcmg.2022.10.021.
[26] B. López, S. Ravassa, M.U. Moreno, G.S. José, J. Beaumont, A. González, J. Díez, Diffuse myocardial fibrosis: mechanisms, diagnosis and therapeutic approaches, Nat. Rev. Cardiol. 18 (2021) 479–498, https://doi.org/10.1038/s41569-020-00504-1.
[27] J.A.C. Lima, D.A. Bluemke, Cardiac abnormalities depicted with MRI in COVID-19: ongoing concern for myocardial injury, Radiology 301 (2021) E371, https://doi.org/10.1148/radiol.2021211492. –E372.